ОБЪЕДИНЕННЫЙ
ИНСТИТУТ
ЯДЕРНЫХ
ИССЛЕДОВАНИЙ
Дубна

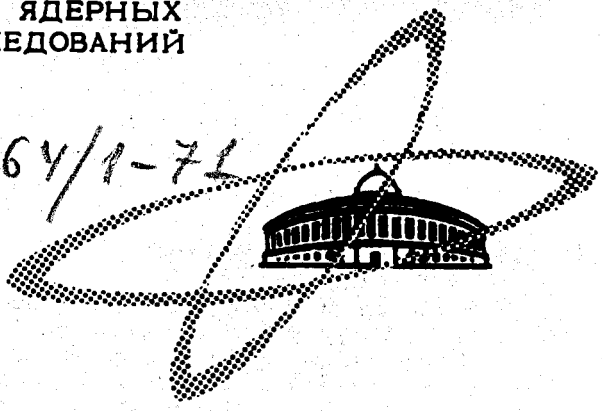

E15 - 5905

B. Kühn , H. Kumpf ,
S. Parzhitsky, S. Tesch

DETERMINATION OF THE NEUTRON-NEUTRON SCATTERING LENGTH FROM A KINEMATICALLY COMPLETE EXPERIMENT WITH THE REACTION ^{3}H (t,n ^{4}He) n

1971

E15 - 5905

B. Kühn*, H. Kumpf*,
S. Parzhitsky, S. Tesch

DETERMINATION OF THE NEUTRON-NEUTRON SCATTERING LENGTH FROM A KINEMATICALLY COMPLETE EXPERIMENT WITH THE REACTION ^{3}H (t,n ^{4}He) n

Submitted *to Nuclear Physics*

* Present adress: Zentralinstitut für Kernforschung, Rossendorf, GDR

1. Introduction

It is well known that the nucleon-nucleon scattering length depends very strongly on the parameters of the potential, depth, interaction radius and core radius. From experimental values of the singlet scattering lengths for the different nucleon pairs a_{nn}, a^s_{np}, and a_{pp} it is possible to learn to what extent the principles of charge independence or charge symmetry are valid. The first principle demands equal nuclear forces in all three possible charge states and consequently $a_{nn} = a^s_{np} = a_{pp}$. Charge symmetry involves only $a_{nn} = a_{pp}$. Only $a^s_{np} = (-23.715 \pm 0.01)$ fm is known with good accuracy[1]. The extraction of the scattering length a_{pp} for scattering on the pure nuclear $p-p$ potential from experimental data is a rather cumbersome procedure, the result of which ($a_{pp} = -17.0$ fm) depends on the details of the assumed nucleon-nucleon potential[2].

So far, attempts to explain the difference $a_{pp} - a^s_{np}$ predict only the correct sign but not its magnitude (see review article ref.[3]). Therefore, knowledge of an accurate value for a_{nn} seems to be of interest. In addition, it is also applied to astrophysics, since the behaviour of neutron matter in neutron stars depends solely on the scattering length a_{nn}.

Up to now, scattering experiments with free neutron targets have not been performed yet. Instead, one is forced to use some many-body nuclear reaction, in which a pair of neutrons is generated. For observation, such events are then selected with two neutrons emerging nearly in the same direction with approximately equal velocities. Experiments with the reactions $^2H(\pi^-,\gamma)2n$ and $^2H(n,2n)p$ have been reported (ref. /4/ and refs. /5,6/, respectively). These are very complicated measurements with extensive experimental techniques. Since the intensity of the incident beams of π^- or neutrons is rather low, the statistical accuracy of the results is limited. Therefore, in recent years ordinary charged particles such as deuterons and tritons have been used to produce neutron pairs in the reactions $^3H(d,^3He)2n$ and $^3H(t,^4He)2n$ (refs. /7,8/ and /9/, respectively).

For the extraction of a_{nn} the experimental data were commonly compared with some kind of Born approximation or the simple, Watson-Migdal formula /10.11/. The latter approximation is valid in the limit of vanishing relative energy of the neutrons. The main aim of the present paper is to provide a kinematically complete experiment with the reaction $^3H(t,n^4He)n$ and use the high yield and favourable experimental possibilities for the extraction of a sufficiently accurate value of a_{nn} from the part of the spectrum with rather small relative energy E_{nn}.

2. Experimental Procedure

The experimental set-up is shown in fig. 1. Tritons from a small Van de Graaff accelerator with energy 1.50MeV bombarded

a gas target with mica entrance and exit windows. The target was filled with gaseous tritium at a pressure of 220 mm Hg by heating uranium loaded with ^3H .After the exposition the gas was reabsorbed by the uranium. The effective length of the target was 13 mm. The beam energy in the target centre was 1.39 MeV. The target was electrically isolated, so that the beam current could be controlled by a current integrator. The beam intensity was limited to 0.3μA rather due to electronic overload than by target failure. The alpha particles were detected at an angle of 10.5^{o}with respect to the beam by means of a p -silicon surface barrier detector. A 4 mg/cm^{2}aluminium absorber placed in front of the detector removed the scattered tritons. The target and alpha detector were surrounded by a reaction chamber with thin walls. The neutron detector consisted of 4x4 cm^2 stilbene scintillator coupled to a fast photomultiplier. It was placed at 162.8^o, coplanar with beam and alpha detector but on the opposite side of the beam (see fig. 1). This geometrical arrangement satisfies the condition that a neutron pair with zero relative energy hits the centre of the scintillator, if an alpha particle passes through the centre of the alpha detector.

The electronic system provided a two-dimensional analysis for the neutron time of flight and the alpha particle energy. The signal from the semiconductor detector was amplified in a preampflier containing a fast and a slow branch[12]. The slow signal is then stored along the Y -axis of a 128x16 channel analyzer. The fast pulses from the preampflier and the signals from the photo-

multiplier anode are fed to a time-to-pulse height converter[13]. Time of flight is then analysed along the X-axis (128 channels). The flight base was 73.3 cm. Pulses from 11th dynode of the phototube were amplified and fed to a discriminator, which gated the analyser. Only the events with proton recoil energy exceeding the threshold of 0.37 MeV were permitted to be analysed. This rather low detection threshold resulted in a wide dynamic range, which was acceptable thanks to a good compensation for the amplitude dependence of trigger time (see ref.[13]). A low threshold for neutron detection has the advantage of minimizing the error in the calculation of the counting efficiency. The parameters of the experimental arrangement such as the diameters of collimators, target and scintillator dimensions, flight base, etc., were roughly optimized in order to get minimal smear-out of the final spectrum at a given efficiency of the system.

3. Experimental Results

3.1. Experiment with the reaction $^3H\,(t, n\,^4He)\,n$

The result of a 25-hour experimental run is shown in fig. 2. There were four groups of events in the experimental two-dimensional distribution, namely:

(I) The leftmost group covers a region where the two neutrons may interact strongly in the final state, as their relative energy is small.

(II) The events in the lower right part originate from sequential decay via the ground state of ^5He.

(III) An intense line in the upper right part with 11.6 MeV neutron energy is generated by the $^2H(t,n)^4He$ reaction with a 0.5% deuterium admixture in the gas of the target.

(IV) A faint line not shown in the figure was explained by the $^3H(d,n)^4He$ reaction by a $(HD)^+$ component in the beam of mass 3.

The last two lines were used to determine the zero point of the time calibration and the time resolution during the actual experiment. The rms-resolution for 11.6 MeV neutrons during 25 hours was 0.78 nsec. The line had no Gaussian shape.

For data reduction the numbers of pulses in the vicinity of the kinematically allowed curve were concentrated on the time axis. The background of accidental coincidences was calculated from the measured single alpha spectrum and the density of chance coincidences in the regions of the plane free of true coincidences. Below the final state interaction peak their contribution amounted only to 2%. The corrected distribution is shown in fig. 3.

For extraction of the scattering length a_{nn} from that spectrum, the measured cross-section $\partial^5\sigma / \partial t_n \partial\Omega_n \partial\Omega_\alpha$ has been compared with the following expression

$$\frac{\partial^5 \sigma}{\partial t_n \, \partial\Omega_n \, \partial\Omega_\alpha} = |T_0|^2 \, B(k_{nn}) \, \rho + A \, f(E_{1\alpha}, E_{2\alpha}) \, \rho \, . \qquad (1)$$

The first term is the Watson-Migdal approximation. Here $|T_0|^2$ denotes the squared matrix element without attractive forces between the neutrons in the final state. The Jost function enhancement factor[14] $B(k_{nn})$ expresses the action of attractive forces in the final state

$$B(k_{nn}) = \left(\frac{r}{2}\right)^2 \frac{\left[k_{nn}^2 + \left(\frac{1}{r} + \sqrt{\frac{1}{r^2} - \frac{2}{r a_{nn}}}\right)^2\right]^2}{k_{nn}^2 + \left(-\frac{1}{a_{nn}} + \frac{r}{2} k_{nn}^2\right)^2}, \qquad (2)$$

where is the effective radius for $n-n$ interaction, $\hbar k_{nn}$ is the relative momentum of the two neutrons. In eq. (1) ρ is the phase space factor, which represents the Jacobian of the transformation from the momenta of three final particles p_{n1}, p_{n2}, p_α to the set of variables fixed or measured in the experiment: the flight time (t_n), neutron and alpha solid angles $(\Omega_n, \Omega_\alpha)$, total energy (E_0) and total momentum (P_0)

$$\rho = \frac{\partial(p_{n1}, p_{n2}, p_\alpha)}{\partial(t_n, \Omega_n, \Omega_\alpha, E_0, P_0)}. \qquad (3)$$

For calculations of kinematical quantities a compilation of formulae published by Ohlsen /15/ was used. The second term in eq. (1) represents the contribution of the reaction mechanism proceeding via ^5He. The function f may be assumed to be constant or be taken in the form found in the experiment with the reaction $^3He(^3He, p\,^4He)p$ (see sect. 3.2). The resulting value of a_{nn} does not depend on the form of f. Before comparing expression (1) with the measured time of flight spectrum $N(t)$ from fig. 3 one must fold in the finite resolutions of the experimental apparatus for neutron angle θ_n, alpha angle θ_α, azimuth ϕ, and time t

$$N(t) = \int \epsilon(t_n) \frac{\partial^5 \sigma}{\partial t_n \partial\Omega_n \partial\Omega_\alpha} F(t_n - t, \theta_n - \theta_{n0}, \theta_\alpha - \theta_{\alpha 0})\, dt_n\, d\theta_n\, d\theta_\alpha\, d\phi. \qquad (4)$$

The index 0 marks the values of the corresponding angles for the centres of the detectors. The resolution function F describes the properties of the measuring equipment. This was very accurately approximated by a four-dimensional Gaussian distribution. The matrix of moments for this distribution was calculated by a Monte-Carlo code, which took into account the dimensions of the target, scintillator and collimators, divergence and diameter of the beam, and multiple scattering in the windows. The integral (eq.(4)) was then calculated numerically by an Hermite quadrature formula. The detection efficiency ϵ of the neutron counter was originally determined by an elaborate program which considered also the double scattering of hydrogen nuclei and successive scattering on carbon and hydrogen as well as the nonlinearity of the light output in stilbene. From this complicated program a simple empirical expression for ϵ in the region of interest was derived. The combination of analytic and probability methods for calculating the integral in eq. (4) proved very effective. Some special calculations showed, that the distortions of the spectrum due to energy inhomogeneity of the beam as well as to the simultaneous absorption of two neutrons in the scintillator were negligible in the considered case.

The following procedure for extracting the value of a_{nn} from the time spectrum of fig. 3 was then adopted. At first, a standard maximum likelihood procedure fitted expression (4) with three free parameters a_{nn}, $|T_0|^2$ and A to the measured distribution in

a broad region. Then the obtained value of A was used to fit two parameters a_{nn} and $|T_0|^2$ in the interval around the maximum corresponding to 0.35 MeV relative energy of the two neutrons. The values for a_{nn} from the two fits differed by only 0.3 fm. The result is

$$a_{nn} = (-15.0 \pm 1.0)\ fm\ . \qquad (5)$$

The standard error ± 1.0 fm includes also the influence of systematic errors in the determination of all experimental quantities. The dominant source of systematic errors were the calibration constants of the time spectrometer, although the channel width was determined by cables, the delay of which was calibrated by means of a precision phasometer. The zero point of the time scale was calculated from the position of the $^2H(t,n)\,^4He$ peak. The pure statistical standard error amounted to 0.3 fm in both the two and three parameter fits. For the unknown effective radius r = 2.7 fm was inserted. But the resulting a_{nn} is almost independent of r .

In fig. 4 some recent results for a_{nn} are compared, which have been obtained on the basis of either complete measurements or the comparison method with the mirror reaction. From the statistical point of view the agreement is even too good. A more extensive review of earlier experiments including single spectrum measurements can be found in ref. 7.

3.2. Expreriment with the mirror reaction $^3He(\,^3He, p\,^3He)\,p$

In order to check the method of obtaining a_{nn} described in the preceding section, an analogous experiment with the mirror

reaction $^3He(^3He, p\,^4He)\,p$ was done. The experimental arrangement was the same as in fig. 1, with the only difference that the time of flight analysis was substituted by pulse height analysis of a proton by means of a second silicon detector. The incident energy of ^3He particles was 3.35 MeV inside the gas target. At lower energies the yield proved to be impracticably low. Fig. 5 demostrates a pulse height spectrum of the protons from a measurement lasting 100 hrs. It was again extracted from a two-dimensional distribution by concentrating counts around the kinematic locus on the E_p axis and subtracting accidental coincidences. A precise energy calibration of the pulse height analyzer was achieved by means of various proton lines from the $^{12}C(^3He, p)$ and $^{16}O(^3He, p)$ reactions. Window thicknesses were determined by observing protons from a CO_2 filling of the target. The distribution of fig. 5 was fitted by an expression similar to eq. (1)

$$\frac{\partial^5\sigma}{\partial E_p\,\partial\Omega_p\,\partial\Omega_\alpha} = |T_0|^2 B(k)\,\rho + A\,f(E_{1\alpha}, E_{2\alpha})\,\rho \quad , \tag{6}$$

with an enhancement factor /18/

$$B(k) = \frac{\left[-\frac{1}{r_0} - \frac{1}{a_{pp}} + \frac{1}{2} r_0 k^2 + \frac{1}{R}\left(\ln\frac{r_0}{R} + 2\gamma + 1\right)\right]^2}{C^2(\eta)\,k^2 + \frac{1}{C^2(\eta)}\left(-\frac{1}{a_{pp}} + \frac{1}{2} r_0 k^2 - \frac{h(\eta)}{R}\right)^2} \,. \tag{7}$$

Here $\hbar k$ is the relative momentum of the two protons, and r_0 and a_{pp} denote the effective radius and scattering length for p–p scattering, respectively. Other quantities are defined by

$$R = \frac{h^2}{M_p e^2} = 28{,}82\,fm\,; \quad \eta = (2kR)^{-1}\,; \quad C^2(\eta) = 2\pi\eta\,/\,(\exp(2\pi\eta) - 1)$$

$$h(\eta) = -\ln - \gamma + \eta^2 \sum_{n=1}^{\infty} \frac{1}{n(n^2+\eta^2)} \qquad (8)$$

where $\gamma = 0.5772$ is Euler's constant.

Since in the case of two protons the enhancement factor B is zero for vanishing relative momentum k, the second term $A f \rho$ from sequential decay via ^5Li is essential. The form of this contribution was determined in an extra measurement with the proton angle changed to $\theta_p = 120^0$. The alpha angle remained unchanged, i.e. $\theta_\alpha = 10.5^0$. In this case the first term of eq. (6) becomes small. It has turned out that the second term could be well described by the simple dependence $f(E_{1\alpha}, E_{2\alpha}) = 1/E_{1\alpha}^2 + 1/E_{2\alpha}^2$, where $E_{i\alpha}$ denotes the energy of relative motion of the proton number i with respect to the alpha particle.

Expression (6) with the known function f is now folded in the manner described in sec. 3.1 and the result is compared with the distribution of fig. 5. The three parameters $|T_0|^2$, a_{pp} and A have been varied. The result obtained for the p–p scattering length is $a_{pp} = (-7.6 \pm 0.6)$ fm. The standard error of 0.6 fm includes systematic errors. The three free parameters are correlated only very weakly. The obtained result agrees well with the exact value $a_{pp} = -7.82$ fm from free p–p scattering.

3.3. Experiment with the reaction $^4He\,(t, p\,^4He)\,n$

For the sake of completeness, we have also measured the two-dimensional p–^4He distribution from the reaction $^3He(t, p\,^4He)\,n$

with triton energy 1.39 MeV inside the target, using the same experimental arrangement as that given in sec. 3.2. The energy calibration has been ensured by reactions of tritons on ^{12}C , ^{16}O and ^{3}He . The proton coincidence spectrum is shown in fig. 6, the measuring time of which was 100 hrs. The following Watson-Migdal expression has been fitted to this experimantal distribution

$$\frac{\partial^5 \sigma}{\partial E_p \, \partial\Omega_p \, \partial\Omega_a} = |T_0^s|^2 B^s(k) \rho + |T_0^t|^2 B^t(k) \rho \quad , \qquad (9)$$

where t and s denote the triplet and singlet $n-p$ states and $B^s(k)$, $B^t(k)$ are Jost function enhancement factors of the form given in eq. (2). Three free parameters have been used in the fitting procedure: the singlet $n-p$ scattering length a_{np}^s and the two intensities $|T_0^s|^2$ and $|T_0^t|^2$. For the other scattering parameters the known values were inserted as follows: $a_{np}^t = 5.41$fm; $r_0^t = 1.75$ fm and $r_0^s = 2.76$ fm. The fits resulted in a value $a_{np}^s = (-21 \pm 3)$ fm in agreement with that found in free $n-p$ scattering [1]. The ratio of the triplet part to the singlet one in the cross-section (eq. (13)) was found to be $|T_0^t|^2 / |T_0^s|^2 = 0.8$.

4. Calculations with Born Approximation

In order to relax some of the assumptions inherent in the Watson-Migdal model, PWBA calculations have been performed. The T -matrix element for our reaction is represented by

$$T = \langle \Phi_a \phi_{n1} \phi_{n2} \phi_{2n\alpha} | V_{n1\alpha} + V_{n2\alpha} + V_{n1n2} | A \Psi^+ \rangle \quad , \qquad (10)$$

where Φ_α is the internal wave function of the alpha particle, and ϕ_{n1}, ϕ_{n2} and $\phi_{2n\alpha}$ describe the relative motions of the respective particles. The interaction potentials between those particles, which separate in the final state, are denoted by $V_{n1\alpha}$, $V_{n2\alpha}$, V_{n1n2}. The antisymmetrization operator A acts on the exact wave function Ψ^+ of six nucleons. Expression (10) may be changed (see, e.g. ref. /14/) to

$$T = < \Phi_\alpha \bar{\phi}_{n1n2} \phi_{2n\alpha} \mid V_{n1\alpha} + V_{n2\alpha} \mid A \Psi^+ > , \qquad (11)$$

where ϕ^-_{n1n2} is one solution of the two-particle Schroedinger equation with interaction V_{n1n2}. In the Born approximation one replaces the exact wave function by the wave function in the entrance channel

$$T = < \Phi_\alpha \phi^-_{n1n2} \phi_{2n\alpha} \mid V_{n1\alpha} + V_{n2\alpha} \mid A \Phi_{t1} \Phi_{t2} \phi_{t1t2} > , \qquad (12)$$

where Φ_{t1}, Φ_{t2} describe the internal states of the tritons and ϕ_{t1t2} their relative motion. The interactions of the neutrons with the alpha particle were represented by a sum of nucleon-nucleon interactions

$$V_{n\alpha} = \sum_{j=1}^{4} V(r_{nj})$$
$$V(r_{nj}) = V_N(r_{nj}) (w + bP^\sigma_{nj} + mP^\tau_{nj} + hP^\tau_{nj} P^\sigma_{nj}) . \qquad (13)$$

For practical calculations the Serber forces ($w = m$; $b = h$) were assumed. For V_N a square well was inserted. For Φ_α and Φ_t the $^1S_0$ and $^1S_{1/2}$ parts with fully symmetric spatial wave functions

of the form given in refs.[16,17] were used. The 15-dimensional integral (eq. (12)) was then calculated with consequent antisymmetrization by a Monte-Carlo procedure. Within the reached statistical accuracy of 5% the result of the PWBA calculation reproduced the form of the Watson-Migdal expression (2).

4. Conclusions

The result of the present measurement for the neutron-neutron scattering length $a_{nn} = (-15.0 \pm 1.0)$ fm agrees with the results of other recent complete experiments within the limits of errors. The $p-p$ and $n-p$ singlet scattering lengths have been extracted from the reactions $^3He(^3He, p\ ^4He)\ p$ and $^3He(t, p\ ^4He)\ n$ in the same manner, using the Watson-Migdal approximation. The comparison with their known values demonstrates the possibility of obtaining accurate nucleon-nucleon scattering parameters in a complete experiment with the nuclear reactions studied.

We are indebted to Prof. F.L. Shapiro and Dr. I.V. Sizov for their stimulating interest and Dr. M. Drazhev for valuable advice in the handling of nanosecond equipment developed by him. We wish to thank Drs. J. Mösner and R. Grötzschel for their contribution to the measurements described in sec. 3.3. We acknowledge, that Prof. N.A. Vlasov has pointed out the feasibility of the reported experiment in 1965, independently from one of us (B.K.).

References

1. H.P. Noyes and H. Fiedelday. In Three Particle Scattering in Quantum Mechanics, ed. by J. Gillespie and J. Nuttal (W.A.Benjamin, New York, 1968).
2. L. Heller, P. Signell and N.R. Yoder. Phys. Rev.Lett., 13, 577 (1964); M.S. Sher, P. Signell and L. Heller. Report of Michigan Univ. Phys.Dept. COO-2061-4.
3. E.M. Henley. In Isospin in Nuclear Physics, ed. by D.H. Wilkinson (North Holland, Amsterdam, 1969).
4. R.P. Haddock, R.M. Salter Jr., M. Zeller, J.B. Czirr and D.R. Nygren. Phys.Rev.Lett., 14, 318 (1965).:;
   R.M. Salter Jr. Thesis, Univ. of California, Technical Report MPG 65-1 (1965),
5. B. Zeitnitz, R. Mashuw and P. Suhr. Nucl.Phys., A149, 449 (1970).
6. H. Grässler and R. Honecker. Nucl.Phys., A136, 446 (1969) and Nucl.Phys., A107, 81 (1968); H. Grässler. Thesis, Aachen, 1968.
7. R. Grötzschel, B. Kühn, K. Möller, J. Mösner and G. Schmidt, to be published.
8. R.J. Slobodrian, H. Meiner, J. Ernst, J.S.C. McKee, H.E. Conzett, A.D. Bacher and F.G. Resmini. Proc. Int. Conf. on the Three-Body Problem, ed. by J.S.C. McKee and P.M. Rolph (North-Holland, Amsterdam, 1970).
9. E.E. Gross, E.V. Hungerford, and J.J. Malanify. Phys.Rev., C1, 1365 (1970).

10. K.M. Watson. Phys.Rev., 88, 1163 (1952).
11. A.B. Migdal. JETP (Sov.Phys.), 1, 2 (1955).
12. M.N. Drazhev and A.I. Ivanenko. JINR, 13-5038, Dubna (1970); M.N. Drazhev and S.S. Parzhitsky. JINR, 3-3466, Dubna (1967).
13. M.N. Drazhev and S.S. Parzhitsky. JINR, 13-5222, Dubna (1970).
14. M.L. Goldberger and K.M. Watson. Collision Thoery (John Wiley and Sons, New York, 1964).
15. G.G. Ohlsen. Nucl.Instr., 37, 240 (1965).
16. J.C. Gunn and J. Irving. Phil.Mag., 42, 1353 (1951); J.Irving. Phil.Mag., 42, 338 (1951).
17. Yu.A. Simonov and A.M. Badalyan. Yadernaya Fizika, 5, 88 (1967).
18. H. Brückmann, W. Kluge, H. Mathäy, L. Schänzler and K. Wick. Report KFK 1172, Karlsruhe(1970).
19. J.P. Nicholson, P.G. Butler, N. Cohen and A.N. James. Phys. Lett., 27B, 452 (1968).

Received by Publishing Department
on June 30, 1971.

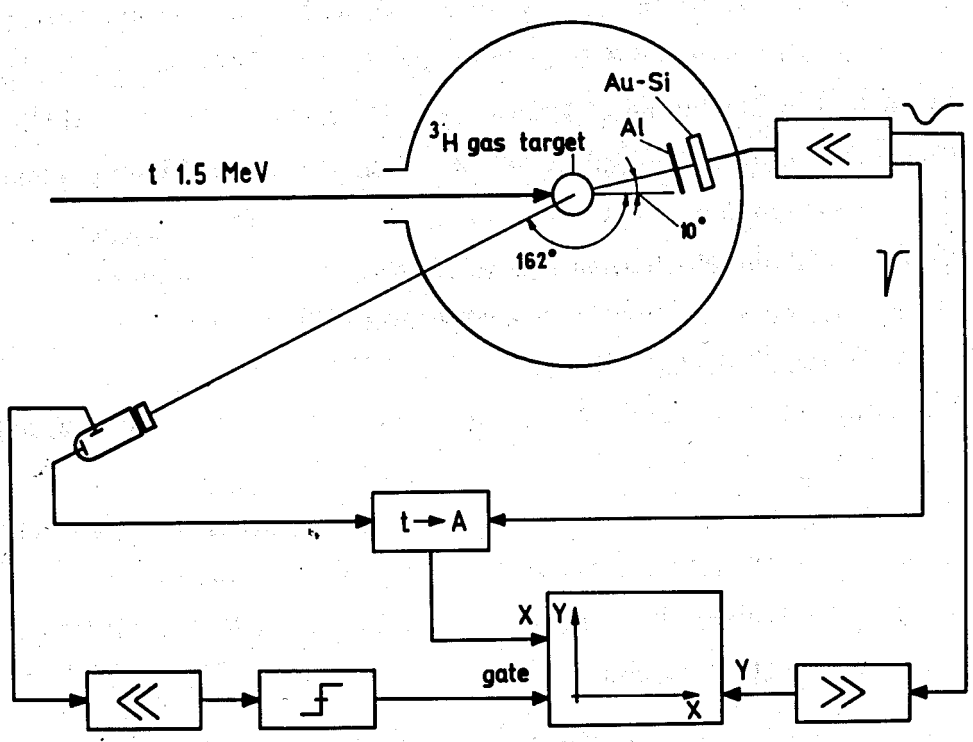

Fig. 1. Experimental arrangement.

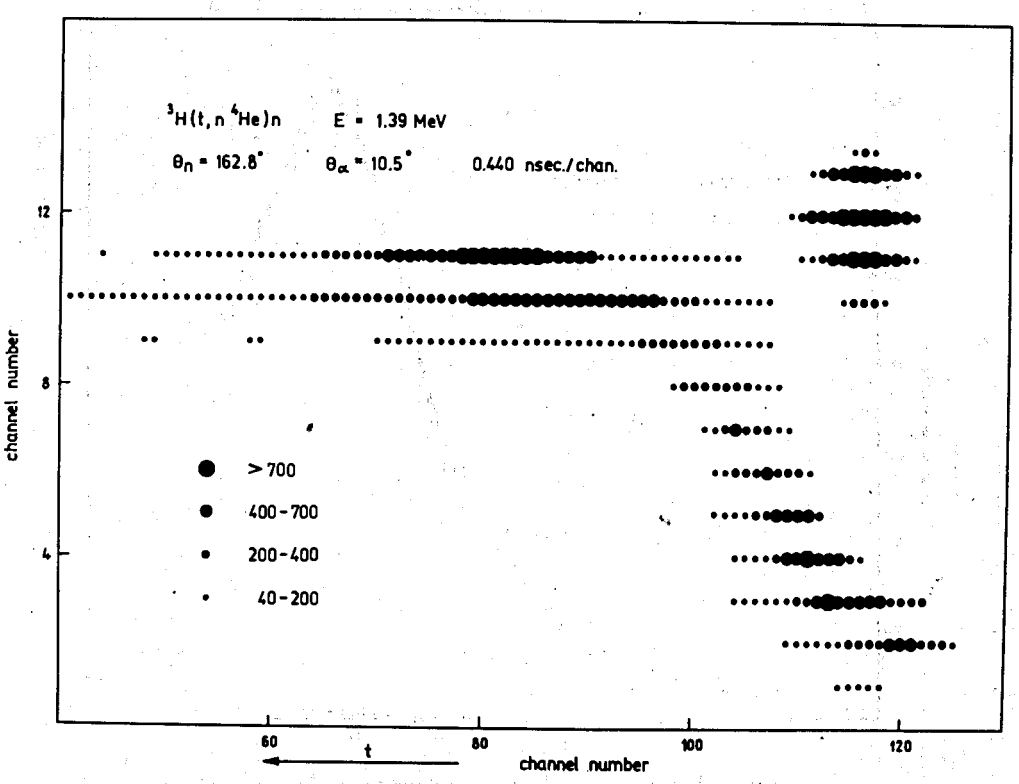

Fig. 2. Two-dimensional distribution from $^3H(t,n\,^4He)\,n$. The neutron time of flight decreases along the axis of abscissa. On the axis of ordinates alpha energy is plotted.

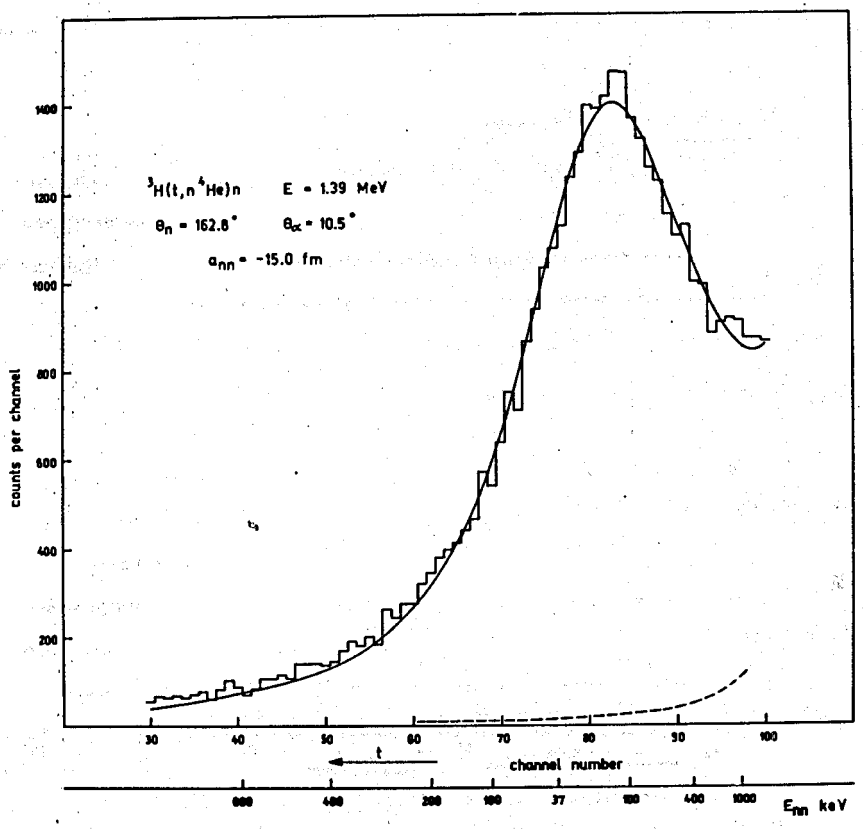

Fig. 3. Neutron time of flight distribution obtained from two-dimensional picture of fig. 2 by concentrating events around the kinematic locus on the time axis. The full line represents the fit by eqs. (1-4). The dashed curve is the contribution of the second terms in eq. (1). The lower scale gives the average relative energy of the two neutrons.

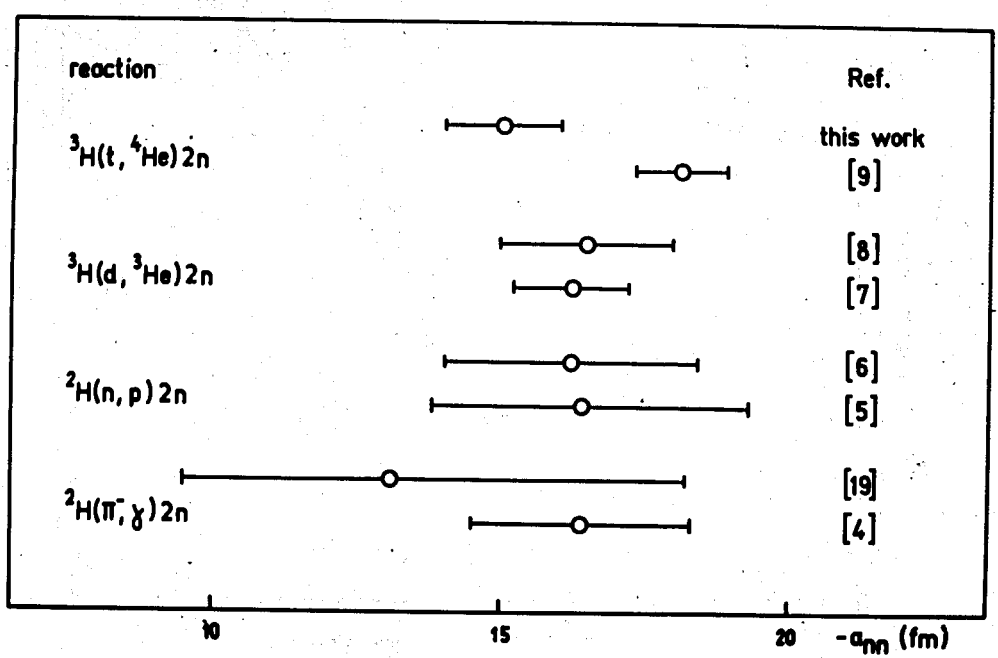

Fig. 4. Comparison with recent measurements of a_{nn}. The error bars represent standard deviations quoted by the authors.

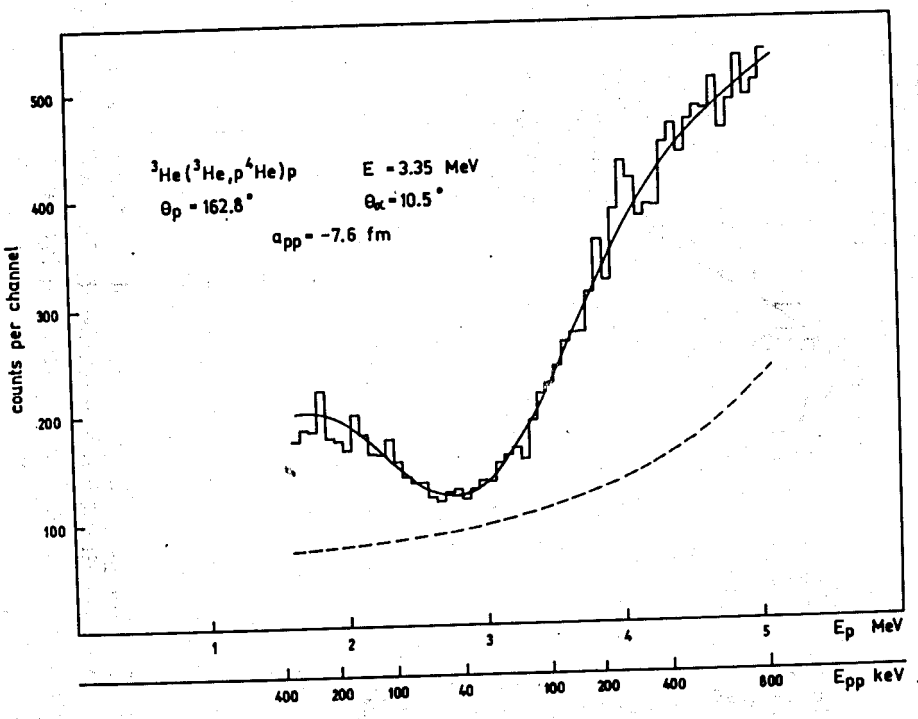

Fig. 5. Pulse height distribution of protons from the reaction $^3He(^3He,p\,^4He)\,p$. The full line represents the fit by eqs. (6-8) folded according to eq. (4). The dashed curve is the contribution of the secons term in eq. (6).

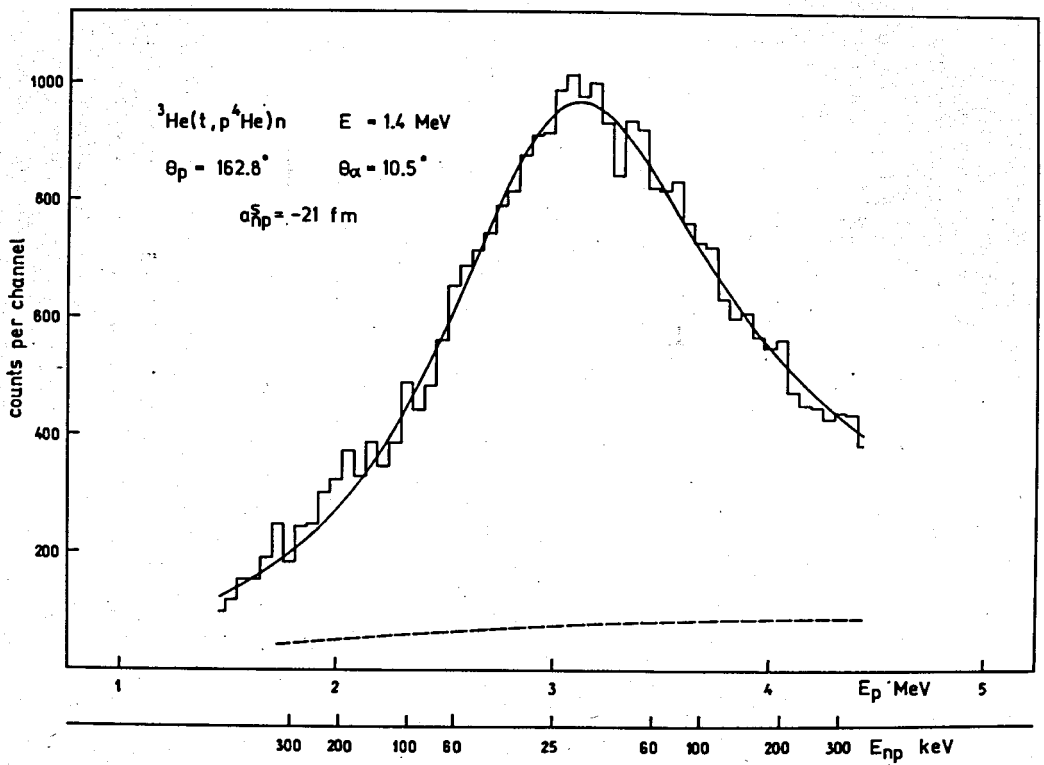

Fig. 6. Pulse height distribution of protons from the reaction $^3He(t,p\,^4He)n$. The full line represents the fit by eq. (9). The dashed curve is the contribution of the triplet term.